**This is a preprint version of the conference paper published in: Proceedings of the ASME 2024 International Mechanical Engineering Congress and Exposition. Volume 10: Mechanics of Solids, Structures, and Fluids; Micro- and Nano-Systems Engineering and Packaging. Portland, Oregon, USA. November 17–21, 2024. V010T13A001. ASME.
https://doi.org/10.1115/IMECE2024-144921

PREPRINT: COMPARISON OF MECHANICAL BEHAVIOR OF MACRO AND MICRO-SIZED ECOFLEX 0030 AND 0031

Ranjith Janardhana
The Department of Mechanical Engineering and Center for High Technology Materials, The University of New Mexico, Albuquerque, NM 87131, USA

Zeynel Guler
Center for High Technology Materials and The Department of Mechanical Engineering, The University of New Mexico, Albuquerque, NM 87131, USA

Fazli Akram
Center for High Technology Materials and The Department of Mechanical Engineering, The University of New Mexico, Albuquerque, NM 87131, USA

Nathan Jackson
The Department of Mechanical Engineering, Center for High Technology Materials, Nanoscience and Microsystems Engineering, The University of New Mexico, Albuquerque, NM 87131, USA

ABSTRACT

Dynamic system applications such as soft robotics, energy harvesters, smart skin, and wearable sensors, require highly stretchable elastomer materials. Ecoflex is a silicone elastomer that is increasing in demand but, the mechanical properties at the micro-scale for Micro Electronic Mechanical Systems (MEMS) are not fully understood. Ecoflex also has different formulations which have varying properties, and the material can be mixed with composites or varying Ecoflex formulations to alter the mechanical properties. In this work, we illustrate the comparison of mechanical properties of micro and macro-sized samples of Ecoflex 0030 and 0031 under uniaxial tensile test. Additionally, the mechanical response of the micro-sized specimens is studied by varying mixing ratios of two different formulations of Ecoflex (0030 and 0031). Material properties of produced samples are investigated by subjecting samples to batch-to-batch repeatability test, cyclic loading, Mullins effect, and stress recovery test. Results demonstrate that the micro-sized samples exhibit higher stiffness in comparison to macro-sized samples. Blending Ecoflex 0030 with higher a concentration of 0031 enhanced the ultimate strength and stretchability of the micro-sized sample in case of 1:3 and 2:3 (0030:0031)

Keywords: Ecoflex, Silicone elastomers, Artificial skin, Elastic modulus, Macro and Micro-scale mechanics.

1. INTRODUCTION

Ecoflex, a silicone elastomer, is gaining popularity as a base material in the development of advanced technology devices for smart material applications [1]. Recently, self-powered soft energy harvesting devices are created using Ecoflex that can be operated under cyclic loading and dynamic operating conditions [2-4]. Biomedical devices have seen significant utilization of Ecoflex to develop artificial skins such as prosthetics, vascular conduits, and arterial phantoms [5, 6]. Ecoflex has also been integrated with liquid metal to create tunable antennas and phase shifters [7-9]. These applications involve materials to be soft, highly flexible/stretchable, thermally stable, adaptable to diverse conditions, and bio-compatible [10-12]. Other applications involve the futuristic development of flexible and stretchable microfluidic devices for the Lab-on-a-chip (LOC) technology for cell separation [13, 14]. Ecoflex is the potentially growing deformable support material in the field of wearable sensors and soft robotics actuators such as stretchable strain sensors for health monitoring [15], dielectric elastomers mimicking artificial muscle [16], and artificial robot skin for tactile sensing [17].

The mechanical behavior of the Ecoflex varies with respect to shore hardness [11, 18], and the selection of the Ecoflex depends on the device application criteria. Soft energy harvesters are intended to sustain dynamic loading and adaptability to environmental conditions [3]. Vascular grafts are designed to have thin, soft material with viscoelastic behavior, large elongation, and biocompatible, so that they mimic functional arteries [5, 19]. Artificial skin sensors and electronic wearable strain sensors require highly soft, elastic (stiffness ranging from 10^2 to 10^7 Pa), durable, and deformable materials which can withstand higher strain rate (> 500%) [17, 20-23]. These transparent epidermal (electronic-skin) are functional to be ultra-stretchable, conformal to skin shape, adhering to the skin's elastic modulus, and ability to withstand a significant stretch over a long period of time [20, 24] in real-world applications.

On the other hand, the miniaturization of smart material devices greatly influences the mechanical properties of the

material compared to the macro-scale [25, 26]. Additionally, previous research observed the inconsistency in the material properties during batch-to-batch fabrication of smart devices [22, 25]. In this regard, we explored the mechanical behavior of the micro and macro-sized Ecoflex 0030 and 0031. To the best of the authors' knowledge, the comparison of material characteristics of micro and macro-sized Ecoflex samples is limited in the literature. In this current study, Ecoflex shore hardness 0030 (Smooth-On Inc., USA) was chosen because it is widely used in SMART material devices [1, 10, 22, 23, 27] and Ecoflex shore hardness 0031 which was 'Near Clear' (transparent) compared to other Ecoflex (Smooth-On, USA). Initially, the paper compares the stress-strain properties of micro and macro-sized Ecoflex samples 0030 and 0031 subjecting them to uniaxial tension. Then characteristics of the fabricated sample were compared under cyclic loading, Mullins effect, stress recovery test, and batch-to-batch repeatability test. Further, the ultimate strength of the blended micro-sized samples (0030:0031) was examined. This work creates the database for the mechanical behavior of Ecoflex shore hardness 0030 and 0031 which guides the type of mixing ratio of Ecoflex to be used for appropriate smart material applications.

2. MATERIALS AND METHODS

2.1 Sample Preparation

The sample preparation procedure was represented in schematic Fig. 1. Initially, two coats of release agent (Ease Release 200) were applied to the 3D printed mold 30 minutes before molding. Part A and B of Ecoflex were weighed in a plastic container in a weight ratio 1:1 (unless specified) using an analytical balance (MTI Corporation, USA). The solution was blended in a speed mixer (FlackTek, Inc.) at a speed of 3000 rpm for 1 minute. Then, the blended solution was slowly poured into the 3D printed mold and smoothed using a doctor blade technique [22]. All the samples were prepared at room temperature. Dimensions of the fabricated macro dogbone shape (in accordance with ASTM-D412-C) and micro dogbone shape were represented in Fig. 2.

The aforementioned procedure was used to prepare different mixing ratios of solution from Ecoflex 0030 and 0031. Mixing ratios were tabulated in Table 1 based on the concentration: 25%, 50%, 75%, and 100%. The entire mixing process cycle consists of primarily mixing Ecoflex 0030 followed by 0031. The effects of mixing Ecoflex formulation in the reverse order were not investigated in this study. Both micro and macro-sized samples were fabricated from the same batch to maintain consistency in the experimental testing.

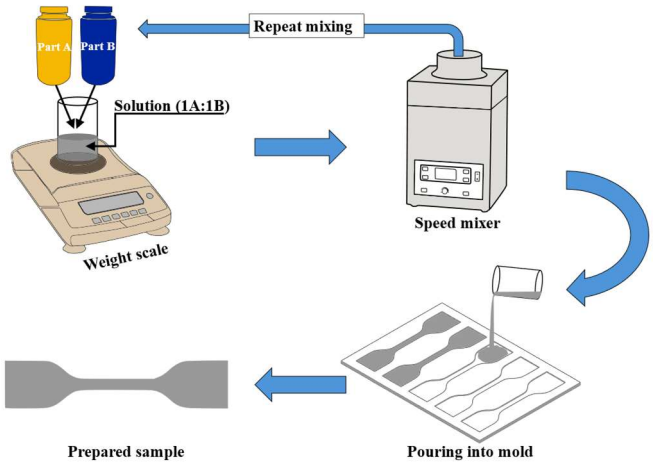

FIGURE 1: SAMPLE PREPARATION SCHEMATIC

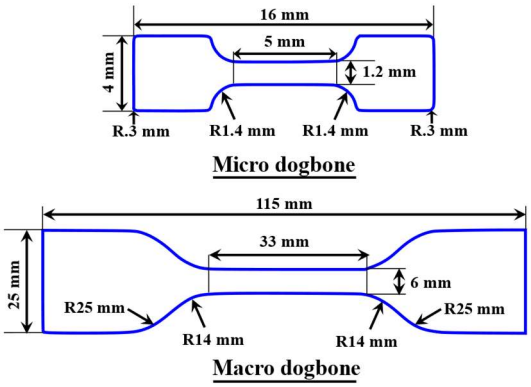

FIGURE 2: DIMENSIONS OF MICRO AND MACRO-SIZED DOGBONE

TABLE 1. ECOFLEX MIXING RATIO.

Ecoflex	Weight ratio	Ecoflex	Weight ratio
0030:0031	1:0	0030:0031	4:3
	0:1		2:3
	1:1		1:3
	3:4		3:2
	1:2		4:1
	1:4		3:1
			2:1

2.2 Characterization Techniques

2.2.1 Mechanical Test:

The mechanical response of the prepared samples was tested and recorded using a Stable Micro Systems texture analysis test frame (TA.XT Plus 100C). The specimens were subjected to uniaxial tensile tests to evaluate the characteristics such as strain softening, cyclic test, and deformation. Stress relaxation of the samples was analyzed by pulling samples up to 600% strain and holding the samples for one hour at strain of 600%. Batch-to-batch samples were tested to examine the feasibility of the manufacturing process. Multiple samples were tested, and average values were obtained at ambient temperature at a speed

of 3 mm/s unless specified. Various types of end strips such as different grits of sandpaper, thick paper, and scour pads (Scotch-Brite) were analyzed to prevent slippage of macro-samples from metallic grip during stretching. However, scour pads were effectively bonded between samples and the metallic grip, which avoided the slippage of samples.

3. RESULTS AND DISCUSSION

3.1 Micro and Macro-Sized Ecoflex 0030 and 0031

3.1.1 Young's modulus:

Micro-sized Ecoflex 0030 was subjected to a cyclic test at the strain of 100% under tension with a speed of 3 mm/s. Stress-strain curve from Fig. 3(a) shows that micro-sized 0030 material retains its original and linear shape after five cycles of loading-unloading tests. Therefore, Young's modulus was calculated within 50% of the initial strain considering the linear region of the curve [24]. The estimated Young's modulus was found to be identical under cyclic loading-unloading as represented in Fig. 3(b). Hereafter, Young's modulus term is used in the context, it would be calculated within 50% of the initial strain.

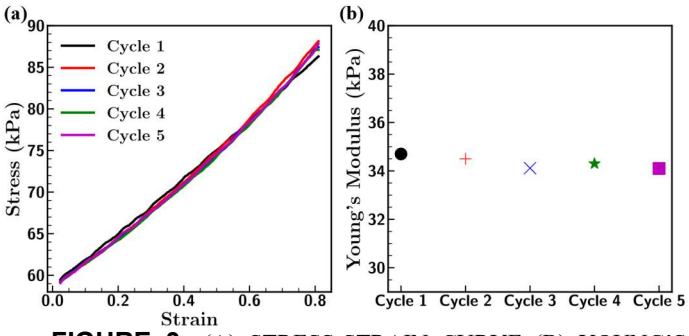

FIGURE 3: (A) STRESS-STRAIN CURVE (B) YOUNG'S MODULU AT 50% OF INITIAL STRAIN FOR MICRO-SIZED ECOFLEX 0030.

3.1.2 Deformation:

Tensile testing was conducted on both micro and macro-sized Ecoflex 0030 and 0031 until fracture. It was observed that micro-sized Ecoflex breaks earlier compared to macro-sized samples as shown in Figs. 4(a) and 4(b). However, micro-sized samples exhibited higher resistance to elongation. Ecoflex 0030 displays higher stretchability in comparison to 0031 in both cases of micro and macro-sized samples depending on the material shore hardness [11]. Furthermore, to investigate the reproducibility of the results, a tensile test was performed by considering 8-10 samples for each case. Based on the results depicted in Fig 4(d), it indicates that the micro-sized samples exhibited larger stiffness compared to the macro-sized samples. The macro-sized samples had a lower Young's modulus range, indicating consistency in the result (Fig 4(d)). In contrast, micro-sized samples had a larger deviation of the stiffness which could be due to the position of samples, slippage from the gripper, variation in the microstructure of the sample, contamination, pre-stress during the demolding process, etc [11]. While these variations in the results were small at the start of the stretch, it increased after a 300% strain as displayed in Fig. 4(c).

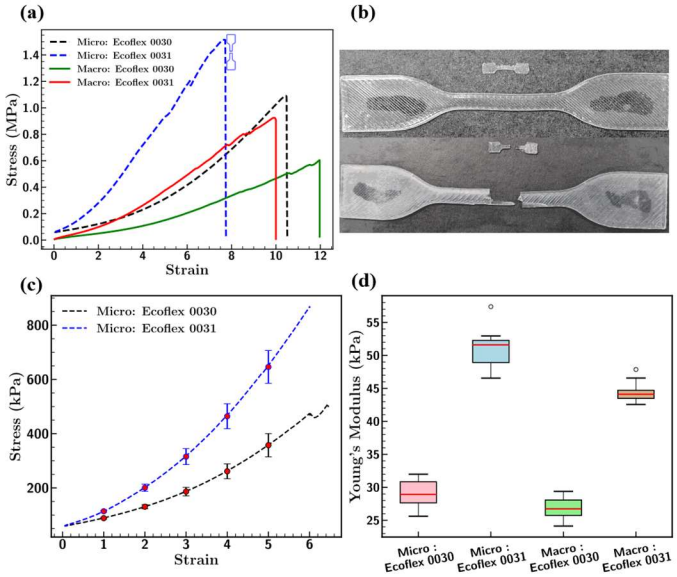

FIGURE 4: (A) COMPARISON OF STRESS-STRAIN CURVE FOR MICRO AND MACRO-SIZED SAMPLES UNTIL FRACTURE; (B) FRACTURE OF MICRO AND MACRO-SIZED SAMPLE 0031; (C) MEAN STRESS-STRAIN CURVE FOR MICRO-SIZED SAMPLE 0030 AND 0031; AND (D) COMPARISON OF YOUNG'S MODULUS OF MICRO AND MACRO-SIZED SAMPLE

3.1.3 Mullins Effect:

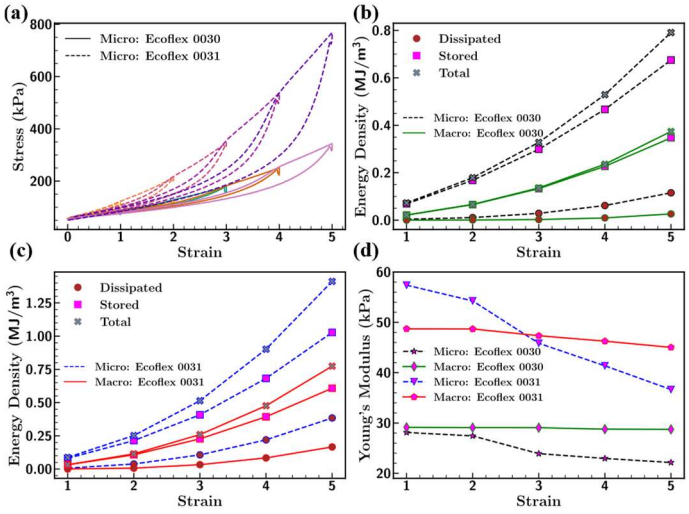

FIGURE 5: (A) STRESS SOFTENING CURVE FOR MICRO-SIZED SAMPLES 0030 AND 0031; (B) AND (C) COMPARISON OF ENERGY DENSITY FOR 0030 AND 0031 SAMPLES RESPECTIVELY; AND (D) YOUNG'S MODULUS UNDER THE MULLINS EFFECT.

Crosslinked silicone elastomers exhibit stress softening or Mullins effect, and these characteristics were analyzed by comparing micro and macro-sized samples by increasing the elongation of the material at different strain rates. Micro-sized

specimens showed the Mullins effects similar to the macro scale under the influence of strain increment as illustrated in Fig. 5(a). Three components of energy density: Dissipated, Stored, and Total energy, increase with stretching of the sample and found hysteretic area highest for the micro-sized sample in comparison to the macro-sized which was obtained under stress-strain curve diagram and represented in Figs. 5(b) and 5(c). It was evident from Fig. 5(a) and 5(d) that the micro-sized sample loses its stiffness significantly under the influence of stretching after a strain of 100%. However, the strain loading-unloading to 500% had less effect on the macro-samples due to its stretchability.

3.1.4 Cyclic:

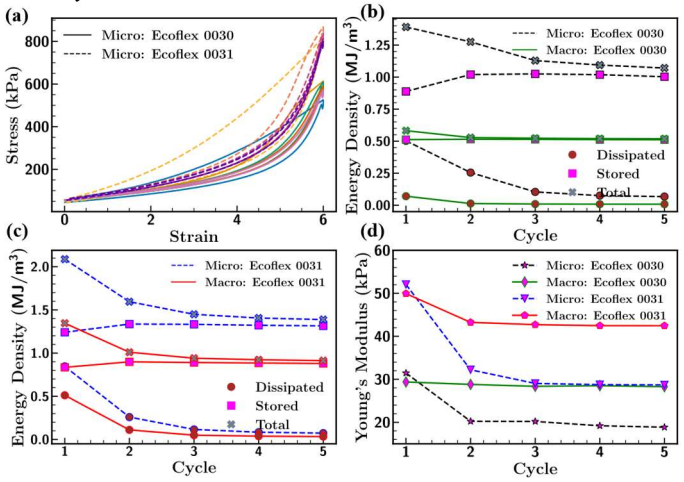

FIGURE 6: COMPARISON OF (A) CYCLIC LOADING CURVE; (B) AND (C) ENERGY DENSITY; AND (D) YOUNG'S MODULUS FOR MICRO AND MACRO-SIZED SAMPLES 0030 AND 0031 UNDER CYCLIC LOADING

Prepared Ecoflex samples were analyzed by applying five cyclic loads at the strain of 600%, since various samples underwent breaking after 600% strain. Each sample displayed an increase in the stress after the first cycle of loading-unloading as illustrated in Fig. 6(a). According to Figs. 6(b) and 6(c), this rise in peak stress at 600% strain was attributed towards the increment in the dissipative energy of the samples. Micro and macro-sized samples show identical cyclic behavior with a decrease in the stored and total energy density. However, the energy density of the macro-sized Ecoflex 0030 remains constant after the second cycle of loading-unloading due to the higher stretchability property. Similarly, insignificant variation in Young's modulus was observed in the case of the macro-sized sample as represented in Fig. 6(d).

3.1.5 Stress Relaxation:

Samples were exposed to stretch at a strain of 600% to understand the material response over a period of one hour. The test was conducted at a strain of 800% and 1000%, however, materials fractured in the case of micro-sized samples. From Fig. 7(a), it was observed that stress reduces at a larger rate for micro-sized samples in comparison to macro-sized samples. These values were tabulated as relaxation ratio in Table 2 by evaluating the maximal stress at zero seconds (600% strain) and final stress after one hour. The relaxation ratio of micro-sized samples depends on the pulling speed of the specimens as it decreases with speed (Table 2).

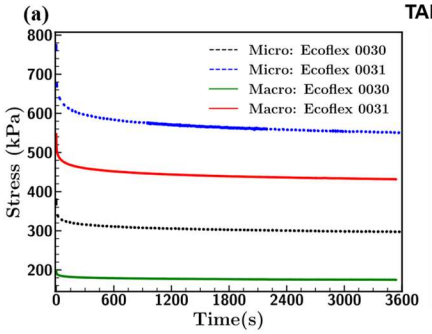

TABLE 2. STRESS RELAXATION

Ecoflex	Speed (mm/s)	Relaxation ratio (%)
Macro: 0030	3	88.31
Macro: 0031	3	78.97
Micro: 0030	0.3	80.62
	3	77.64
	30	71.01
Micro: 0031	0.3	74.44
	3	70.32
	30	68.46

FIGURE 7: COMPARISON OF (A) STRESS RELAXATION

3.2 Mixture of Micro-Sized Ecoflex 0030 and 0031

Different ratios of blended micro-sized Ecoflex were pulled at the strain rate of 3 mm/s and results were presented in a series of plots. Young's modulus was found to be maximum for the Ecoflex ratio 0:1 (0030:0031) (i.e. for 0031 with an average of 51 kPa) and minimum for 1:0 (i.e. for 0030 with an average of 30 kPa) as depicted in Fig. 8(a).

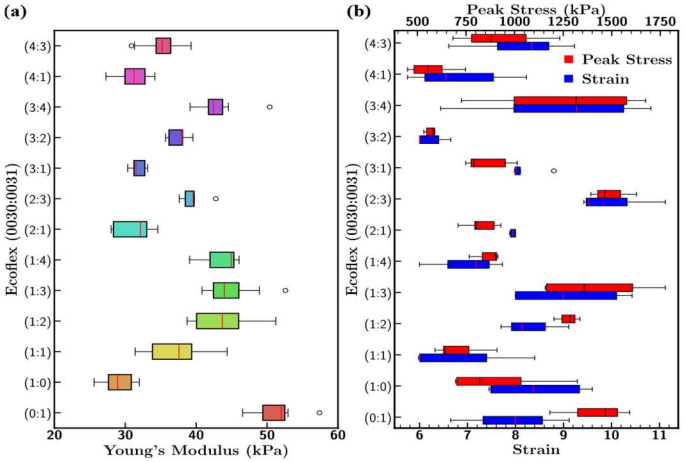

FIGURE 8: COMPARISON OF (A) INITIAL YOUNG'S MODULUS; AND (B) PEAK STRESS AND STRAIN FOR MIXED RATIO SOLUTION.

The Young's modulus falls between 0030 and 0031 for other mixing ratios of 0030:0031. Adding every part of 0031 contributes towards increasing the initial stiffness of the blended solution for ratios 1:1, 1:2, 1:3, and 1:4. On contrast higher concentrations of 0030 decrease the initial stiffness as seen for ratios 2:1, 3:2, and 4:1. However, outcomes of breaking stress from Fig. 8(b) shows that the initial Young's modulus property had an insignificant impact on the ultimate strength of the blended solution. Larger peak stress (> 1.25 MPa) and higher stretchability (> 1000%) were observed for 1:3, 2:3, and 3:4 ratios. Nevertheless, the ultimate strength and stretchability of

the blended solution were increased by the addition of 0031 up to certain concentrations.

Figure 9 displays the stress-strain diagram for the blended solution of 0030:0031 up to a strain of 500%. The upper and lower boundaries of the resultant spectrum (Fig. 9) were bounded by Ecoflex 0031 and 0030 respectively. Mixture ratio 1:1 divides the portion of the outcomes at the center, where adding concentration 0031 falls above ratio 1:1 (shown by '--') and adding concentration 0030 below ratio 1:1 (shown by '-.'). The behavior of the blended ratios 1:1 and 4:3 was identical to each other up to 400% strain, however material characteristics for 4:3 deviate after 400% strain. It may be worth noting that in this section the results were analyzed by considering 7-8 samples for each mixture ratio.

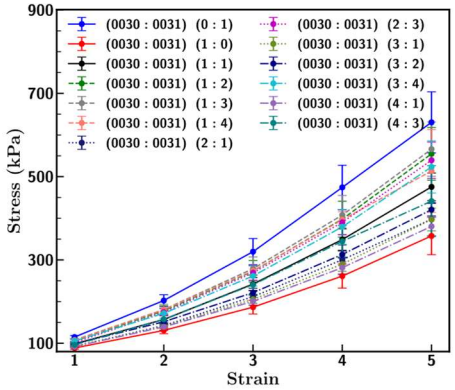

FIGURE 9: MEAN STRESS-STRAIN CURVE FOR BLENDED SOLUTION UP TO 500% STRAIN

3.3 Batch Fabrication

The manufacturing feasibility of micro-sized samples was investigated by fabricating the Phase 2 samples after twenty days from Phase 1. Phase 2 mixture samples were randomly selected. Figure 10 indicates the experiment findings of Phase 1('-', solid line) and Phase 2 ('--', dash line) samples through a stress-strain diagram. Results suggest that the behavior of samples prepared from Phase 1 and Phase 2 were similar in the case of 0030 (1:0) and 0031 (0:1). However, materials characteristics were significantly impacted for the blended solution as shown in Fig. 10 and Table 3. Factors affecting this deviation may include minor variations in the concentration of the mixing solution, differences in the amount of time to complete the fabrication process and demolding process.

4. CONCLUSION

The results illustrate that micro-scale Ecoflex are stiffer and have less elongation to break than macro-scale using the same manufacturing process. Mixing the Ecoflex 0030 and 0031 improved the stretchability and ultimate strength of the material. Batch-to-batch test results showed the deviation in the outcomes of Phase 1 and Phase 2 findings for the blended solution. Hence, the method of manufacturing the materials has a significant influence on the mechanical properties, such as mixing procedures and concentration over the micro-sized samples. The results presented in this paper will aid researchers in designing MEMS devices using Ecoflex and demonstrate how mixing multiple formulations of Ecoflex can be used to fine-tune mechanical properties to meet specifications.

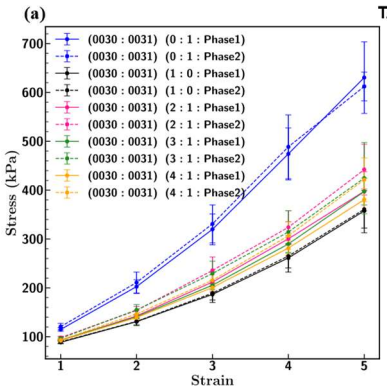

TABLE 3. STRESS RELAXATION.

Ecoflex Micro 0030:0031	Phase	Relaxation ratio (%)
1:0	Phase 1	71.01
	Phase 2	71.25
0:1	Phase 1	70.32
	Phase 2	70.79
2:1	Phase 1	77.07
	Phase 2	73.255
4:1	Phase 1	74.64
	Phase 2	70.27

FIGURE 10: BATCH-TO-BATCH TESTING OF THE MICRO-SIZED BLENDED SOLUTION

ACKNOWLEDGEMENTS

The project was partially funded by the Research Allocation Committee at University of New Mexico and partially funded by Army Research Office and Air Force Office of Scientific Research under Grant Number W911NF-23-1-0171.

REFERENCES

[1] J. Vaicekauskaite, P. Mazurek, S. Vudayagiri, and A. L. Skov, "Mapping the mechanical and electrical properties of commercial silicone elastomer formulations for stretchable transducers," (in en), *J. Mater. Chem. C,* vol. 8, no. 4, pp. 1273-1279, 2020 2020, doi: 10.1039/C9TC05072H.

[2] B. Kim, D. Y. Hyeon, and K.-I. Park, "Stretchable Energy Harvester Based on Piezoelectric Composites and Kirigami Electrodes," *Journal of the Korean Institute of Electrical and Electronic Material Engineers,* vol. 36, no. 5, pp. 525-530, 2023/09/01/ 2023, doi: 10.4313/JKEM.2023.36.5.14.

[3] M. Mariello, L. Fachechi, F. Guido, and M. De Vittorio, "Multifunctional sub-100 μm thickness flexible piezo/triboelectric hybrid water energy harvester based on biocompatible AlN and soft parylene C-PDMS-Ecoflex™," (in en), *Nano Energy,* vol. 83, p. 105811, 2021/05// 2021, doi: 10.1016/j.nanoen.2021.105811.

[4] X. Zhang, J. Ai, Y. Yue, Y. Shi, R. Zou, and B. Su, "Anti-stress ball energy harvester," (in en), *Nano Energy,* vol. 90, p. 106493, 2021/12// 2021, doi: 10.1016/j.nanoen.2021.106493.

[5] O. Byrne, F. Coulter, E. T. Roche, and E. D. O'Cearbhaill, "In silico design of additively manufacturable composite synthetic vascular conduits and grafts with tuneable compliance," (in en), *Biomater. Sci.,* vol. 9, no. 12, pp. 4343-4355, 2021 2021, doi: 10.1039/D0BM02169E.

[6] D. Zhalmuratova *et al.*, "Mimicking "J-Shaped" and Anisotropic Stress–Strain Behavior of Human and Porcine Aorta by Fabric-Reinforced Elastomer Composites," (in

en), *ACS Appl. Mater. Interfaces,* vol. 11, no. 36, pp. 33323-33335, 2019/09/11/ 2019, doi: 10.1021/acsami.9b10524.

[7] F. Nikbakhtnasrabadi, H. El Matbouly, M. Ntagios, and R. Dahiya, "Textile-based stretchable microstrip antenna with intrinsic strain sensing," *ACS Applied Electronic Materials,* vol. 3, no. 5, pp. 2233-2246, 2021.

[8] D. M. Hensley, C. G. Christodoulou, and N. Jackson, "A stretchable liquid metal coaxial phase shifter," *IEEE Open Journal of Antennas and Propagation,* vol. 2, pp. 370-374, 2021.

[9] N. Jackson, J. Buckley, C. Clarke, and F. Stam, "Manufacturing methods of stretchable liquid metal-based antenna," *Microsystem Technologies,* vol. 25, pp. 3175-3184, 2019.

[10] J. Lavazza, M. Contino, and C. Marano, "Strain rate, temperature and deformation state effect on Ecoflex 00-50 silicone mechanical behaviour," (in en), *Mechanics of Materials,* vol. 178, p. 104560, 2023/03// 2023, doi: 10.1016/j.mechmat.2023.104560.

[11] Z. Liao, M. Hossain, and X. Yao, "Ecoflex polymer of different Shore hardnesses: Experimental investigations and constitutive modelling," (in en), *Mechanics of Materials,* vol. 144, p. 103366, 2020/05// 2020, doi: 10.1016/j.mechmat.2020.103366.

[12] J. T. B. Overvelde *et al.*, "Mechanical and electrical numerical analysis of soft liquid-embedded deformation sensors analysis," (in en), *Extreme Mechanics Letters,* vol. 1, pp. 42-46, 2014/12// 2014, doi: 10.1016/j.eml.2014.11.003.

[13] R. D. Janardhana and N. Jackson, "A Simulated Investigation of Lithium Niobate Orientation Effects on Standing Acoustic Waves," (in en), *Sensors,* vol. 23, no. 19, p. 8317, 2023/10/08/ 2023, doi: 10.3390/s23198317.

[14] M. Sun, X. Zhou, Y. Quan, L. Zhang, and Y. Xie, "Highly flexible elastomer microfluidic chip for single cell manipulation," (in en), *Biomicrofluidics,* vol. 16, no. 2, p. 024104, 2022/03/01/ 2022, doi: 10.1063/5.0086717.

[15] S. Kumbay Yildiz, R. Mutlu, and G. Alici, "Fabrication and characterisation of highly stretchable elastomeric strain sensors for prosthetic hand applications," (in en), *Sensors and Actuators A: Physical,* vol. 247, pp. 514-521, 2016/08// 2016, doi: 10.1016/j.sna.2016.06.037.

[16] Z. Ye, M. S. S. Faisal, R. Asmatulu, and Z. Chen, "Artificial muscles of dielectric elastomers attached to artificial tendons of functionalized carbon fibers," in *SPIE Smart Structures and Materials + Nondestructive Evaluation and Health Monitoring*, Y. Bar-Cohen, Ed., 2014/03/26/ 2014, San Diego, California, USA, p. 905616, doi: 10.1117/12.2047212. [Online]. Available: http://proceedings.spiedigitallibrary.org/proceeding.aspx?doi=10.1117/12.2047212

[17] P. Yong-Lae, C. Bor-Rong, and R. J. Wood, "Design and Fabrication of Soft Artificial Skin Using Embedded Microchannels and Liquid Conductors," *IEEE Sensors J.,* vol. 12, no. 8, pp. 2711-2718, 2012/08// 2012, doi: 10.1109/JSEN.2012.2200790.

[18] Z. Liao, J. Yang, M. Hossain, G. Chagnon, L. Jing, and X. Yao, "On the stress recovery behaviour of Ecoflex silicone rubbers," (in en), *International Journal of Mechanical Sciences,* vol. 206, p. 106624, 2021/09// 2021, doi: 10.1016/j.ijmecsci.2021.106624.

[19] G. Soldani *et al.*, "Long term performance of small-diameter vascular grafts made of a poly(ether)urethane–polydimethylsiloxane semi-interpenetrating polymeric network," (in en), *Biomaterials,* vol. 31, no. 9, pp. 2592-2605, 2010/03// 2010, doi: 10.1016/j.biomaterials.2009.12.017.

[20] M. Amjadi, Y. J. Yoon, and I. Park, "Ultra-stretchable and skin-mountable strain sensors using carbon nanotubes–Ecoflex nanocomposites," *Nanotechnology,* vol. 26, no. 37, p. 375501, 2015/09/18/ 2015, doi: 10.1088/0957-4484/26/37/375501.

[21] I. Apsite, S. Salehi, and L. Ionov, "Materials for Smart Soft Actuator Systems," (in en), *Chem. Rev.,* vol. 122, no. 1, pp. 1349-1415, 2022/01/12/ 2022, doi: 10.1021/acs.chemrev.1c00453.

[22] J. C. Case, E. L. White, and R. K. Kramer, "Soft Material Characterization for Robotic Applications," (in en), *Soft Robotics,* vol. 2, no. 2, pp. 80-87, 2015/06// 2015, doi: 10.1089/soro.2015.0002.

[23] K. Shimizu, T. Nagai, and J. Shintake, "Dielectric Elastomer Fiber Actuators with Aqueous Electrode," (in en), *Polymers,* vol. 13, no. 24, p. 4310, 2021/12/09/ 2021, doi: 10.3390/polym13244310.

[24] T. Nishikawa, H. Yamane, N. Matsuhisa, and N. Miki, "Stretchable Strain Sensor with Small but Sufficient Adhesion to Skin," (in en), *Sensors,* vol. 23, no. 4, p. 1774, 2023/02/04/ 2023, doi: 10.3390/s23041774.

[25] S. Akbari and H. R. Shea, "An array of 100μm×100μm dielectric elastomer actuators with 80% strain for tissue engineering applications," (in en), *Sensors and Actuators A: Physical,* vol. 186, pp. 236-241, 2012/10// 2012, doi: 10.1016/j.sna.2012.01.030.

[26] Z. Guler and N. Jackson, "Mechanical Properties of Stretchable Multifunctional Ecoflex Composites for E-Skin Applications," in *ASME 2023 International Mechanical Engineering Congress and Exposition*, 2023/10/29/ 2023, New Orleans, Louisiana, USA: American Society of Mechanical Engineers, p. V012T13A020, doi: 10.1115/IMECE2023-117258. [Online]. Available: https://asmedigitalcollection.asme.org/IMECE/proceedings/IMECE2023/87691/V012T13A020/1196254

[27] D. R. Darby, Z. Cai, C. R. Mason, and J. T. Pham, "Modulus and adhesion of Sylgard 184, Solaris, and Ecoflex 00-30 silicone elastomers with varied mixing ratios," (in en), *J of Applied Polymer Sci,* vol. 139, no. 25, p. e52412, 2022/07/05/ 2022, doi: 10.1002/app.52412.